Hindawi Publishing Corporation
Advances in Condensed Matter Physics
Volume 2012, Article ID 951976, 5 pages
doi:10.1155/2012/951976

Research Article

Micromagnetic Study of Synchronization of Nonlinear Spin-Torque Oscillators to Microwave Current and Field

M. Carpentieri,[1] G. Finocchio,[2] A. Giordano,[2] B. Azzerboni,[2] and F. Lattarulo[3]

[1] *Dipartimento di Elettronica, Informatica e Sistemistica, University della Calabria, Via P. Bucci 42C, 87036 Rende, Italy*
[2] *Dipartimento di Fisica della Materia e Ingegneria Elettronica, University degli studi di Messina, C.da di Dio, 98100 Messina, Italy*
[3] *Dipartimento di Elettrotecnica ed Elettronica, Politecnico di Bari, Via Orabona 4, 70125 Bari, Italy*

Correspondence should be addressed to M. Carpentieri, mcarpentieri@deis.unical.it

Received 30 March 2012; Revised 17 July 2012; Accepted 23 July 2012

Academic Editor: Giancarlo Consolo

The nonautonomous dynamics of spin-torque oscillators in presence of both microwave current and field has been numerically studied in nanostructured devices. When both microwave current and field are applied at the same frequency, integer phase locking at different locking ratio is found. In the locking region, a study of the intrinsic phase shift between the locking force (current or field) and the giant magnetoresistive signal as a function of the bias current is also exploited.

1. Introduction

In the last years, the effects due to a direct transfer of the spin angular momentum [1–4] in nanomagnets (magnetization reversal [5, 6] or persistent oscillation of the magnetization [7, 8]) have opened new perspectives in the field of nanotechnology. In particular, one of the most promising applications is the possibility to obtain a competitive generation of nanoscale microwave oscillators, namely, spin-transfer torque oscillators (STOs) [9, 10]. Nowadays, STO is promising from a technological point of view being one of the smallest auto-oscillators observed in nature. It exhibits properties such as frequency tunability on bias current and field and narrow linewidth. To find practical application, STOs have to improve their output power. Some years ago, some researchers demonstrated that synchronized oscillators provided increased output power [11, 12]. This effect, which is receiving a great deal of attention due to its potential applications in telecommunications, has been studied both experimentally and theoretically for the purpose of understanding and realizing mutual synchronization between two or more STOs for microwave source applications. Later, other studies showed the synchronization of serially connected STOs governed by phase locking to a microwave current offering a valid approach to fabricate STOs for output power levels closer to 1 μW [13, 14].

The synchronization phenomenon is based on the well-known property that when the external frequency f_{RF} of a "weak" microwave current or field is close to the free running oscillation frequency f_0 of the STO, the self-oscillation mode moves and locks to the external frequency. Locking phenomena are also present for the ratio $r = f_{RF}/f_0$ close to all integers ($r = 1, 2, 3$, etc.) and several rational values [15].

We recently studied the injection locking phenomenon based on the application of a microwave field on perpendicular materials [16]. These systems mainly operate under "weak" microwave signal regime (the power of the microwave signal is negligible compared to the self-oscillation one) [9, 16–18].

In this work, by means of a micromagnetic study, the nonautonomous dynamical behavior of STO in presence of microwave signal composed by the simultaneous application of microwave current density J_{AC} and field h_{AC} (both at the same frequency) is studied. Also, the influence of a static field on the frequency behavior is investigated.

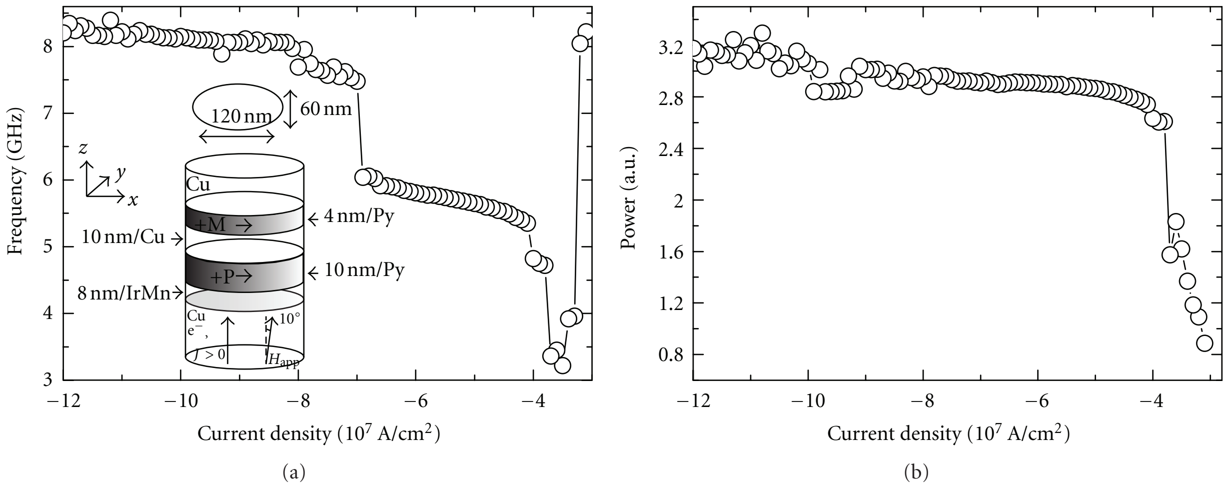

FIGURE 1: (a) Frequency and (b) power amplitude versus dc current density when an out-of-plane field of 250 mT tilted 10° versus x-directionis applied. No microwave source is applied. Inset of (a): sketch of the structure.

2. Device and Numerical Details

We studied the dynamical behavior of exchange bias spin-valves composed by IrMn(8 nm)/Py(10 nm) (polarizer)/Cu(10 nm)/Py(4 nm) (free layer) with elliptical cross-sectional area (120 nm × 60 nm) (see inset of Figure 1(a)). A Cartesian coordinate system has been introduced, where the x- and the y-axes are, respectively, related to the easy and hard in-plane axes of the ellipse. Our numerical experiment is based on the numerical solution of the Landau-Lifshitz-Gilbert-Slonczweski (LLGS) equation [1–3]. In addition to the standard effective field (external, exchange, and self-magnetostatic), the Oersted field and the magnetostatic coupling with the polarizer are taken into account. The resulting equation (LLG + S) is expressed as

$$\frac{d\mathbf{m}}{d\tau} = -\,\mathbf{m}\times\mathbf{h}_{\text{eff}} + \frac{\alpha}{M_s}\left(\mathbf{m}\times\frac{d\mathbf{m}}{d\tau}\right) - \chi\mathbf{m}\times(\mathbf{m}\times\mathbf{p}), \quad (1)$$

where $\mathbf{m} = \mathbf{M}/M_S$ and $\mathbf{h_{eff}} = \mathbf{H_{eff}}/M_S$ are the dimensionless magnetization vector and the effective field, respectively, $\tau = \gamma_0 M_s t$ is the dimensionless time, γ_0 is the gyromagnetic ratio, and M_s is the saturation magnetization of the free layer. The first term on the right-hand side of (1) represents the precessional torque around the effective field, whereas the second one is the phenomenological dissipation term, α being the so-called Gilbert parameter. The third term in (1) is the dimensionless Slonczewski spin-transfer torque, where $\mathbf{p} = \mathbf{P}/M_s$ represents the dimensionless magnetization in the pinned layer, and the prefactor χ is given by

$$\chi = \frac{\mu_B}{\gamma_0}\frac{J_{\text{app}}}{M_s^2 ed}g(\mathbf{m},\mathbf{p}), \quad (2)$$

where e and μ_B are the electric charge and the Bohr magneton respectively, J_{app} is the current per unit area (density current), and d is the thickness of the free layer, and $g(m,p)$ is the polarization function depending on the relative orientation of the magnetizations [1–3].

For a complete model description of the numerical techniques see also [19–22]. Typical parameters for the Py have been used: saturation magnetization $M_S = 650 \times 10^3$ A/m, exchange constant $A = 1.3 \times 10^{-11}$ J/m, damping parameter $\alpha = 0.02$, and polarization factor $\eta = 0.3$ [1–3]. The bias field is applied out-of-plane (z-direction) with a tilted angle of 10° along the x-axis. The polarizer is considered fixed along the x-direction. To study the locking, we consider a microwave current $J_{\text{RF}} = J_M \sin(2\pi f_{\text{AC}}t + \pi/2)$ ($J_M \le 2 \times 10^7$ A/cm^2) and a microwave field linearly polarized at $\pi/4$ in the x-y plane $h_{\text{RF}} = h_M \sin(2\pi f_{\text{AC}}t + \pi/4)\hat{x} + h_M \sin(2\pi f_{\text{AC}}t + \pi/4)\hat{y}$ ($h_M \le 3$ mT). This microwave field can be generated by using the experimental technique developed in [25]. All the computations have been performed with no thermal effects.

3. Micromagnetic Results and Discussion

In order to characterize the device behavior, first of all we analyzed the STO in the free running regime. We observe dynamical regime in a wide range of current density for bias field larger than 180 mT. Here we discuss in detail data for a bias field of 250 mT, but qualitative similar results have been also observed for 200 and 300 mT.

In order to characterize the oscillator regime of the device, we swapped the dc current exceeding the critical current value (to obtain dynamics regime, threshold current density was $J = 3 \times 10^7$ A/cm^2) up to current values, where oscillation regime is degraded by noise. Frequency and power behavior of the nano-oscillator with respect to the current density is shown in Figures 1(a) and 1(b) (no microwave signal). The frequency curve f_0 as a function of J presents red shift from the critical current up to $J_1 = -3.5 \times 10^7$ A/cm^2, where the dynamics is characterized by an in-plane oscillation axis. For $|J| > |J_1|$ the magnetization precesses around an out-of-plane axis and the blue shift is achieved. The discontinuities observed in the oscillation frequency are related to jumps of the oscillation axis that

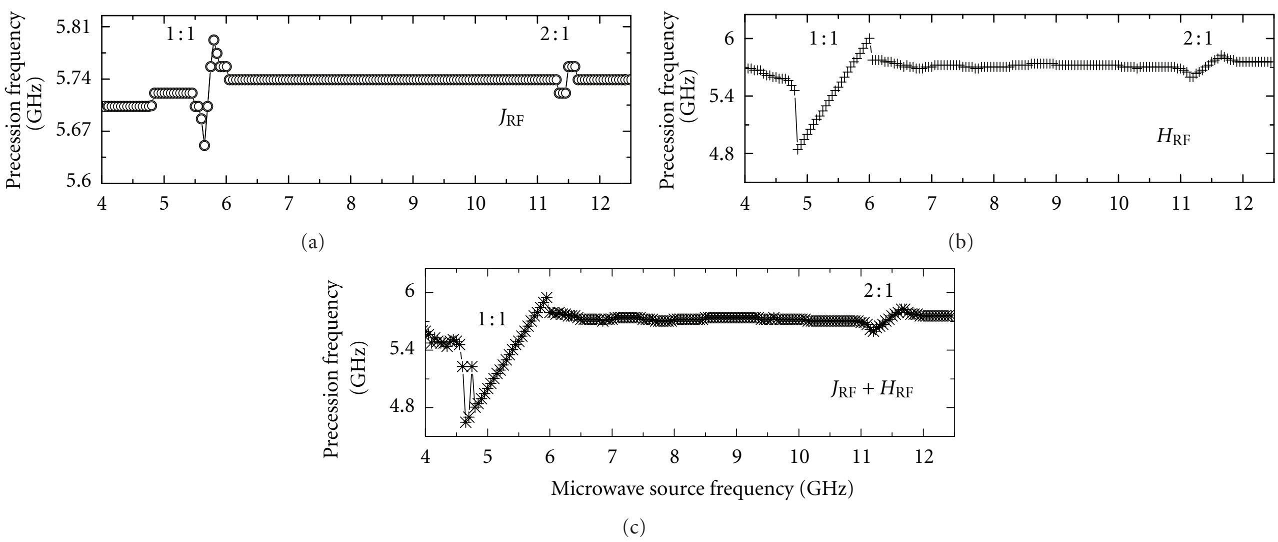

Figure 2: Response of the STO self-oscillation for $H_{DC} = 250$ mT and $J_{DC} = -5\times10^7$ A/cm^2 as a function of the microwave source frequency when (a) $J_{RF} = 2\times10^7$ A/cm^2, (b) $H_{RF} = 1$ mT, and (c) RF current $J_{RF} = 1\times10^7$ A/cm^2 and RF field $H_{RF} = 1$ mT are applied together at the same frequency. The locking regions for the frequency ratio of 1 : 1 and 2 : 1 are also visible.

correspond to transitions between strongly nonlinear oscillation modes. Similar discontinuities have been also observed in some experimental work [23]. In addition, we performed micromagnetic simulations increasing the out-of-plane static field up to 600 mT, and we observed that for out-of-plane bias field larger than 400 mT the red-shift zone disappears, jumps are softer, and the synchronization data achieved are similar to results already published in the literature (see e.g., [10] for a review). At larger field (>600 mT), the polarizer is moved from the x-direction towards the out-of-plane z-direction that might generate additional noise showing not coherent precessional states.

Figure 1(b) shows the power versus current behavior. Nonlinear power strongly increases at low current and for current values greater than 4×10^7 A/cm^2 is about constant.

We systematically studied the locking to the first harmonic (the same of the self-oscillation) in the blue shift region as a function of the J_M and h_M. Figure 2 shows the precession frequency of the GMR signal as a function of the microwave source frequency in two cases: RF current only and RF current and field together (for $H_{DC} = 250$ mT and $J_{DC} = -5\times10^7$ A/cm^2). We found different locking regions at the locking ratio 1 : 1, 2 : 1, and 3 : 1 (in the last case only when the microwave field component is applied, not shown here). Typically, the locking region is much larger when the microwave force is a field (or a combination of current and field). In fact, in the case of current we found a locking region of about 150 MHz (1 : 1) and 50 MHz (2 : 1), whereas no locking on the third harmonic is found. Microwave field provides a locking region larger than 1 GHz and, since driving force breaks the oscillation symmetry, the 1 : 1 synchronization region has a specific asymmetric shape. Then, whereas for small forcing signal the synchronization region can be described by an analytical theory (symmetric tongue where the locking region increases linearly with force amplitude) [24], it cannot be described analytically when increasing the forcing signal and their precise determination requires necessarily specific numerical techniques.

Figure 3(a) summarizes the Arnold tongue ($J = -5\times10^7$ A/cm^2) computed up to $J_M = 1\times10^7$ A/cm^2 ($h_M = 0$ mT) and then increasing h_M up to 3 mT with $J_M = 1\times10^7$ A/cm^2 held unchanged. The border lines have been computed considering the lower (in the left part) and higher (in the right part) microwave frequency where the phase locking is achieved. In the low regime of microwave source, the Arnold tongue is related to the only application of the microwave current, which can be considered as a "weak" microwave signal. In fact, such a signal gives rise to symmetric synchronization region (no hysteresis is observed) with a locking band linearly dependent on the force locking.

When both microwave current and field are applied simultaneously at the same frequency, the nonautonomous response becomes more complicated. The presence of an additional weak microwave field gives rise to increasing of the locking region from 150 MHz at $h_M = 0$ mT to 1.3 GHz for $h_M = 1$ mT. As can be observed the locking region is strongly asymmetric. This is caused by the strong nonlinearity of the dependence of the auto-oscillation frequency on the oscillation power [25].

Figure 3(b) shows the phase difference between the magnetization oscillation and the microwave source (negative angle means magnetization in delay with respect to microwave source, Ψ being the phase of the natural precession of the magnetization and Ψ_e the force phase) when the microwave component is applied at the same frequency of the free precession one. As shown, typically in both cases (microwave field or current), the phase increases with current and decreases after a maximum value. The phase shift depends on the initial detuning, and it goes to

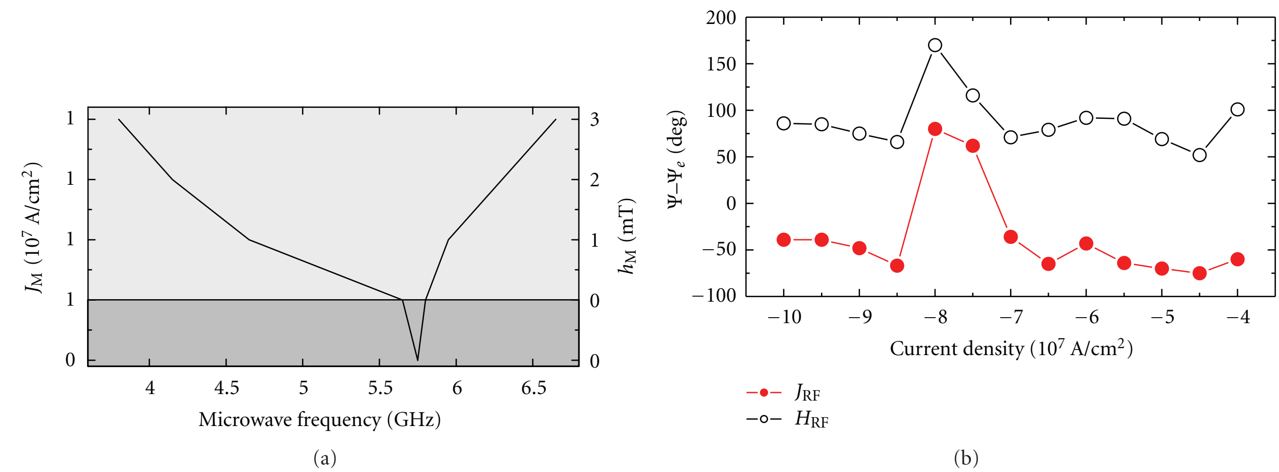

FIGURE 3: (a) Arnold tongue computed for $H_{DC} = 250$ mT and $J = -5 \times 10^7$ A/cm^2 varying the magnitude of RF current and field. (b) Phase difference between external force (current or field) and output magnetization as a function of dc current when an RF source at the same frequency of the free precessional one is applied. Filled-red circle: RF current, white circle: RF field.

zero only if there is no detuning, that is, in the center of the synchronization region. It should be remembered that the phase difference depends on the initial phase of the force and the way it affects the oscillator. We emphasize here that the phase locking implies that phase difference will be kept bounded inside a finite range of detuning, that is, within the synchronization region. In this case the microwave current and field give the same qualitative behavior to the oscillator, but the phase difference is translated by an angle of about 120°. As expected, phase difference between microwave source and the magnetization precession follows the frequency behavior. It initially decreases with dc current amplitude (precession frequency decreases) and then increases with dc current (precession frequency increases) up to current values of the order of 7×10^7 A/cm^2. After that current value, phase shift jumps about 180°, typically this is due to the different oscillation mode from in-plane to out-of-plane mode. Lastly, the phase difference gradually increases following the frequency slow rising with dc current magnitude [26].

In the locking region an intrinsic phase shift Ψ_i, computed as the difference between the phase of the self-oscillation Ψ and the phase of the microwave current Ψ_e, is found.

Figure 4 summarizes Ψ_i as a function of the microwave frequency, as can be observed a linear relationship between Ψ_i and f_{AC} is achieved with a range of Ψ_i which can cross 0 or $\pi/2$ depending on the bias current density. As reported by Slavin and Tiberkevich [10], analytical formulation of the phase difference in the locking region is given by

$$\Phi_0 = \arcsin\left(\frac{f_{AC} - f_0}{\Delta f}\right) - \arctan(\upsilon), \tag{3}$$

where $\upsilon = (N/(G_+ - G_-))$ is the nonlinear frequency shift. We found N which is characterized from two different values of nonlinear frequency shift $N = 2\pi(df/dp)$, p is the oscillation power, and G_+ and G_- are the non-linear

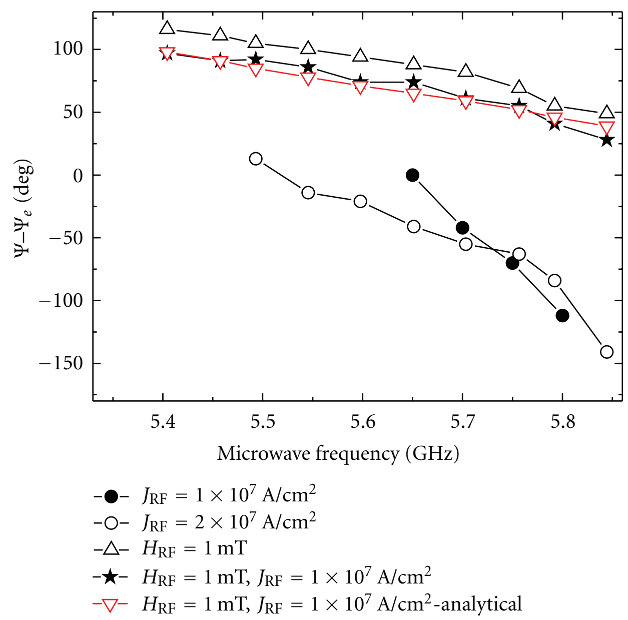

FIGURE 4: Intrinsic phase shift Ψ_i between the phase of self-oscillation and microwave source (current or field) in the locking region for $J_{DC} = 5 \times 10^7$ A/cm^2.

damping coefficients as in [10]. Phase difference is strongly dependent on the frequency in the locking region [27]. For all the cases, the phase difference decreases from left to right in the Arnold tongue. In particular, the slope of the curve is strong for RF current locking whereas it is more soft for RF field, a result also in substantial agreement with the analytical theory. Considering (3) for RF applied field, the locking bandwidth and nonlinear frequency shift are larger with respect to ac current. A good agreement between analytical and numerical data is found.

4. Conclusions

In summary, we have studied micromagnetically the nonlinear behavior of spin-torque nano-oscillators in locking regime driven by microwave current and field. We found a large locking region at different harmonics when RF field is applied. The effect of the static applied field is also studied. Finally, we showed and explained the intrinsic phase shift due to the difference between microwave source and magnetization precession inside the locking region, also comparing our numerical data with a recent analytical theory.

Acknowledgments

This paper was supported by Spanish Project under Contract no. MAT2011-28532-C03-01. The authors would like to thank Sergio Greco for his support with this paper.

References

[1] J. C. Slonczewski, "Current-driven excitation of magnetic multilayers," *Journal of Magnetism and Magnetic Materials*, vol. 159, no. 1-2, pp. L1–L7, 1996.

[2] J. C. Slonczewski, "Excitation of spin waves by an electric current," *Journal of Magnetism and Magnetic Materials*, vol. 195, no. 2, pp. L261–L268, 1999.

[3] J. C. Slonczewski, "Currents and torques in metallic magnetic multilayers," *Journal of Magnetism and Magnetic Materials*, vol. 247, no. 3, pp. 324–338, 2002.

[4] L. Berger, "Emission of spin waves by a magnetic multilayer traversed by a current," *Physical Review B*, vol. 54, no. 13, pp. 9353–9358, 1996.

[5] I. N. Krivorotov, N. C. Emley, J. C. Sankey, S. I. Kiselev, D. C. Ralph, and R. A. Buhrman, "Time-domain measurements of nanomagnet dynamics driven by spin-transfer torques," *Science*, vol. 307, no. 5707, pp. 228–231, 2005.

[6] D. C. Ralph and M. D. Stiles, "Spin transfer torques," *Journal of Magnetism and Magnetic Materials*, vol. 320, no. 7, pp. 1190–1216, 2008.

[7] S. I. Klselev, J. C. Sankey, I. N. Krivorotov et al., "Microwave oscillations of a nanomagnet driven by a spin-polarized current," *Nature*, vol. 425, no. 6956, pp. 380–383, 2003.

[8] A. A. Tulapurkar, Y. Suzuki, A. Fukushima et al., "Spin-torque diode effect in magnetic tunnel junctions," *Nature*, vol. 438, no. 7066, pp. 339–342, 2005.

[9] W. H. Rippard, M. R. Pufall, S. Kaka, S. E. Russek, and T. J. Silva, "Direct-current induced dynamics in $Co_{90}Fe_{10}/Ni_{80}Fe_{20}$ point contacts," *Physical Review Letters*, vol. 92, no. 2, Article ID 027201, 4 pages, 2004.

[10] A. Slavin and V. Tiberkevich, "Nonlinear auto-oscillator theory of microwave generation by spin-polarized current," *IEEE Transactions on Magnetics*, vol. 45, no. 4, pp. 1875–1918, 2009.

[11] S. Kaka, M. R. Pufall, W. H. Rippard, T. J. Silva, S. E. Russek, and J. A. Katine, "Mutual phase-locking of microwave spin torque nano-oscillators," *Nature*, vol. 437, no. 7057, pp. 389–392, 2005.

[12] F. B. Mancoff, N. D. Rizzo, B. N. Engel, and S. Tehrani, "Phase-locking in double-point-contact spin-transfer devices," *Nature*, vol. 437, no. 7057, pp. 393–395, 2005.

[13] J. Grollier, V. Cros, and A. Fert, "Synchronization of spin-transfer oscillators driven by stimulated microwave currents," *Physical Review B*, vol. 73, no. 6, Article ID 060409(R), 4 pages, 2006.

[14] W. H. Rippard, M. R. Pufall, S. Kaka, T. J. Silva, S. E. Russek, and J. A. Katine, "Injection locking and phase control of spin transfer nano-oscillators," *Physical Review Letters*, vol. 95, no. 6, Article ID 067203, pp. 1–4, 2005.

[15] S. Urazhdin, P. Tabor, V. Tiberkevich, and A. Slavin, "Fractional synchronization of spin-torque nano-oscillators," *Physical Review Letters*, vol. 105, no. 10, Article ID 104101, 4 pages, 2010.

[16] M. Carpentieri, G. Finocchio, B. Azzerboni, and L. Torres, "Spin-transfer-torque resonant switching and injection locking in the presence of a weak external microwave field for spin valves with perpendicular materials," *Physical Review B*, vol. 82, no. 9, Article ID 094434, 8 pages, 2010.

[17] G. Consolo, V. Puliafito, G. Finocchio et al., "Combined frequency-amplitude nonlinear modulation: theory and applications," *IEEE Transactions on Magnetics*, vol. 46, no. 9, pp. 3629–3634, 2010.

[18] R. Bonin, G. Bertotti, C. Serpico, I. D. Mayergoyz, and M. D'Aquino, "Analytical treatment of synchronization of spin-torque oscillators by microwave magnetic fields," *European Physical Journal B*, vol. 68, no. 2, pp. 221–231, 2009.

[19] A. Romeo, G. Finocchio, M. Carpentieri, L. Torres, G. Consolo, and B. Azzerboni, "A numerical solution of the magnetizationreversal modeling in a permalloy thin film using fifth order Runge-Kutta method with adaptive step size control," *Physica B*, vol. 403, no. 2-3, pp. 464–468, 2008.

[20] E. Martinez, L. Torres, L. Lopez-Diaz, M. Carpentieri, and G. Finocchio, "Spin-polarized current-driven switching in permalloy nanostructures," *Journal of Applied Physics*, vol. 97, no. 10, Article ID 10E302, 3 pages, 2005.

[21] Martinez et al., "standard problem #4 report," The free layer has been discretized in computational cells of $5 \times 5 \times 4\,\mathrm{nm}^3$. The time step used was 32 fs, http://www.ctcms.nist.gov/~rdm/mumag.org.html.

[22] M. Carpentieri, L. Torres, B. Azzerboni, G. Finocchio, G. Consolo, and L. Lopez-Diaz, "Magnetization dynamics driven by spin-polarized current in nanomagnets," *Journal of Magnetism and Magnetic Materials*, vol. 316, no. 2, pp. 488–491, 2007.

[23] I. N. Krivorotov, D. V. Berkov, N. L. Gorn et al., "Large-amplitude coherent spin waves excited by spin-polarized current in nanoscale spin valves," *Physical Review B*, vol. 76, no. 2, Article ID 024418, 14 pages, 2007.

[24] P. Maffezzoni, "Computing the synchronization regions of injection-locked strongly nonlinear oscillators for frequency division applications," *IEEE Transactions on Computer-Aided Design of Integrated Circuits and Systems*, vol. 29, no. 12, pp. 1849–1857, 2010.

[25] P. Tabor, V. Tiberkevich, A. Slavin, and S. Urazhdin, "Hysteretic synchronization of nonlinear spin-torque oscillators," *Physical Review B*, vol. 82, no. 2, Article ID 020407, 4 pages, 2010.

[26] Y. Zhou, J. Persson, S. Bonetti, and J. Akerman, "Tunable intrinsic phase of a spin torque oscillator," *Applied Physics Letters*, vol. 92, no. 9, Article ID 092505, 3 pages, 2008.

[27] G. Finocchio, G. Siracusano, V. Tiberkevich, I. N. Krivorotov, L. Torres, and B. Azzerboni, "Time-domain study of frequency-power correlation in spin-torque oscillators," *Physical Review B*, vol. 81, no. 18, Article ID 184411, 6 pages, 2010.